Pharm Res (2012) 29:2419–2431
DOI 10.1007/s11095-012-0768-7

RESEARCH PAPER

Dynamic Analysis of GI Absorption and Hepatic Distribution Processes of Telmisartan in Rats Using Positron Emission Tomography

Makoto Kataoka • Tadayuki Takashima • Tomotaka Shingaki • Yoshinobu Hashidzume • Yumiko Katayama • Yasuhiro Wada • Hiroyuki Oh • Yoshie Masaoka • Shinji Sakuma • Yuichi Sugiyama • Shinji Yamashita • Yasuyoshi Watanabe

Received: 27 December 2011 / Accepted: 25 April 2012 / Published online: 23 May 2012

ABSTRACT

Purpose To dynamically analyze the processes of oral absorption and hepatobiliary distribution of telmisartan using positron emission tomography (PET).

Methods ^{11}C-labeled telmisartan ([^{11}C]TEL) was orally administered to rats with or without non-radiolabeled telmisartan (0.5, and 10 mg/kg). PET scanning of abdominal region and whole body was performed under conscious condition. *In situ* intestinal closed loop study in rats and *in vitro* permeation study in MDR1-MDCK II cell monolayers were also conducted.

Results After oral administration of [^{11}C]TEL, systemic bioavailability and hepatic distribution of radioactivity increased non-linearly with dose. In the intestinal lumen, both telmisartan and its glucuronide were detected and the ratio of telmisartan decreased dramatically at high dose of telmisartan. *In situ* closed loop study showed most of telmisartan-glucuronide detected in the intestinal lumen was derived from the bile excretion. In addition, *in vitro* permeation study revealed that telmisartan is a substrate of P-glycoprotein.

Conclusion PET imaging analysis successfully demonstrated the processes of intestinal absorption and hepatic distribution of telmisartan. PET study combined with appropriate *in situ* and *in vitro* experiments is highly expected to be a potent tool for better understanding of GI absorption and subsequent tissue distribution of various drugs and drug candidates.

KEY WORDS molecular imaging · oral absorption · positron emission tomography (PET) · telmisartan · transporter

INTRODUCTION

A trend methodology of drug discovery in pharmaceutical industries has produced an increased frequency of drug candidates having poor oral bioavailability (BA) and/or undesirable pharmacokinetic (PK) properties (1). Those candidates often show insufficient therapeutic effect and drop out in the process of development including clinical trials, although they intrinsically possess high pharmacological activity or high affinity to the target molecules (2).

As one of the predominant factors of drug BA/PK, important roles of drug transporters are now widely recognized. BA of drugs after oral administration (F_{oral}) is expressed as;

$$F_{oral} = F_a \times F_g \times F_h$$

where F_a is a fraction of absorbed from the gastrointestinal (GI) tract, and F_g and F_h are fractions not undergo the intestinal and the hepatic first-pass metabolism, respectively.

M. Kataoka • T. Takashima • T. Shingaki • Y. Hashidzume • Y. Katayama • Y. Wada • Y. Watanabe
RIKEN Center for Molecular Imaging Science
6-7-3 Minatojima minamimachi, Chuo-ku
Kobe, Hyogo 650-0047, Japan

M. Kataoka • H. Oh • Y. Masaoka • S. Sakuma • S. Yamashita (✉)
Faculty of Pharmaceutical Sciences, Setsunan University
45-1 Nagaotoge-cho
Hirakata, Osaka 573-0101, Japan
e-mail: shinji@pharm.setsunan.ac.jp

T. Shingaki
ADME Research Inc.
1-12-8 Senba-higashi
Minoh, Osaka 562-0035, Japan

Y. Sugiyama
Graduate School of Pharmaceutical Sciences
The University of Tokyo
7-3-1 Hongo
Bunkyo-ku, Tokyo 113-0033, Japan

F_a of various drugs is profoundly affected by influx and/or efflux transporters, facilitating or obstructing the membrane permeation, expressed at the intestinal epithelial cells (3,4). After absorbed into the portal blood flow, the extent of hepatic first pass metabolism of drugs (E_h=1-F_h) is determined not only by the affinity to the metabolic enzymes but also by the hepatobiliary uptake and excretion processes in which various transporters are involved. In case of drugs to be a substrate of various transporters, therefore, assessment of oral BA and subsequent tissue distribution is supposed to be complicated and require quantitative considerations on the interaction with each transporter and enzyme at the GI tract and the liver.

Telmisartan is a potent angiotensin receptor blocker (ARB) having a high affinity to angiotensin II type 1 receptors and is used for the treatment of hypertension (5). Since the half-life of telmisartan in elimination phase of human (20 h) is significantly longer than that of other ARB (e.g. 2 h for losartan, 6 h for valsartan), this drug shows a long duration of action (6,7). In addition, telmisartan is known to distribute to the liver selectively, undergo the phase II metabolism by UDP-glucuronosyltransferases to form telmisartan-O-acyl-glucuronide (8), and then telmisartan-O-acyl-glucuronide is rapidly excreted into the bile that accounts for about 10 % of its systemic exposure (9). Ishiguro *et al.* have revealed that OATP1B3 expressed in hepatocytes mainly mediated the hepatocellular uptake of telmisartan. Moreover, telmisartan was extensively glucuronidated in the liver and then excreted into the bile as a glucuronide by MRP2 as well as by P-gp and breast cancer resistant protein (BCRP). (10,11). Therefore, to fully understand the series of oral absorption processes of telmisartan into the systemic circulation, PK analysis only with the plasma concentration-time profile after oral administration is thought to be insufficient.

Positron emission tomography (PET) is now widely used for diagnosis of various diseases, mostly for early detection of tumor (12,13). Since PET can visualize the disposition of positron-emitting radionuclides in the body *in vivo,* it is engaged at many of pharmaceutical companies for the PK analysis of drug candidates. So far, PET has been utilized to visualize the distribution of drugs into the brain on human where roles of drug transporters such as P-gp in the blood–brain barrier were quantitatively evaluated *in vivo* (14). In the previous report, we have successfully demonstrated the GI absorption process of ^{18}F-labeled 2-fluoro-2-deoxy-D-glucose ([^{18}F]FDG) after oral administration to rats, by scanning abdominal region and whole-body with PET (15). It was concluded that PET technology is quite useful not only to investigate the tissue distribution of probes injected intravenously, but also to elucidate the oral drug absorption process *in vivo*.

In this study, PET technology was applied for investigating GI absorption and hepatobiliary transport processes of telmisartan. ^{11}C-labeled telmisartan ([^{11}C]TEL) was orally administered to rats with or without non-radiolabeled telmisartan and abdominal region and whole body were scanned by PET. In addition, in order to consider the mechanisms of non-linear absorption of telmisartan, *in situ* intestinal closed loop and *in vitro* drug transport experiments were performed.

MATERIALS AND METHODS

Materials

N-desmethyl telmisartan was kindly provided by Boehringer Ingelheim Pharma GmbH & Co. KG (Biberach, Germany). Telmisartan and telmisartan-O-acyl-glucuronide, were purchased from Sigma-Aldrich (St. Louis, MO). Isoflurane (ESCAIN®) was purchased from Mylan pharmaceuticals. MDCK II cells expressing MDR1 (a P-gp-coded gene) were kindly provided by Dr. Piet Borst (The Netherlands Cancer Institute). Minimum Essential Medium Alpha Medium with L-glutamine, ribonucleosides, and deoxyribonuculeosides (MEMAM), non-essential amino acids (NEAA, 10 mM), fetal bovine serum (FBS), L-glutamine (200 mM), trypsin-EDTA (trypsin: 0.25 %, EDTA: 1 mM), and antibiotic-antimycotic (penicillin: 10,000 U/mL, streptomycin: 10 mg/mL, amphotericin B: 25 μg/mL; dissolved in 0.85 % NaCl aqueous solution) were purchased from Gibco Laboratories (Lenexa, KS). Cell culture inserts with polyethylene terephthalate filters (pore size: 1.0 μm, growth area: 0.9 cm^2) were obtained by Becton Dickinson Bioscience (Bedford, MA). All other chemicals were commercial products of reagent grade. All other materials were used without further purification.

Synthesis of ^{11}C-labeled Telmisartan

^{11}C-labeled telmisartan ([^{11}C]TEL, Fig. 1) was automatically prepared from N-desmethyl telmisartan methyl ester afforded by esterification of N-desmethyl telmisartan with trimethylsilyldiazomethane. The requisite [^{11}C]incorporated methyl iodide was prepared from [^{11}C]carbon dioxide via reaction with lithium aluminum hydride and subsequent treatment with hydriodic acid according to the established method (16,17). Carbon-11-labeled methyl iodide was typically reacted with 2.3 mg of N-desmethyl telmisartan methyl ester and 5.0 mg of KOH (powdered) in 250 μL of dimethyl sulfoxide (DMSO) for 5 min at 80 °C. One molar of NaOH (200 μL) was added to the mixture, the resultant mixture was heated at 100 °C for 3 min, followed by the treatment with 400 μL of acetic acid for 4 min. The crude product was purified on a preparative COSMOSIL®

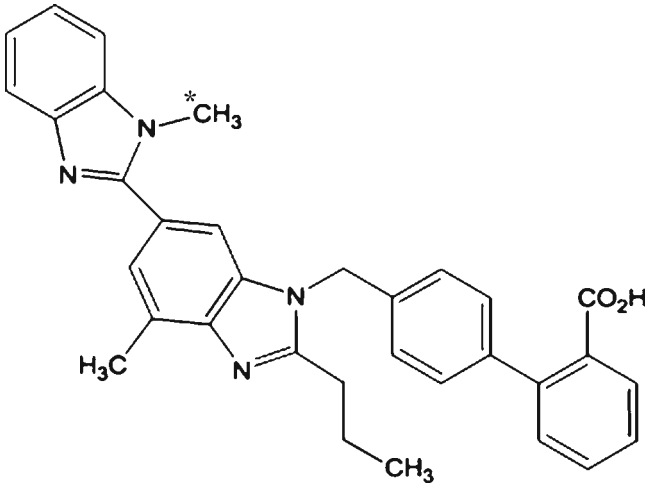

Fig. 1 Chemical structure of [^{11}C]TEL. The asterisk denotes the position of the ^{11}C-label.

Cholester column (5 μ, 250 mm×10 mm i.d., Nacalai Tesque, Kyoto, Japan) with 55 v/v% of acetonitrile in ammonium acetate (10 mM, adjusted at pH 4.5 by the addition of formic acid). After evaporation of the HPLC solvent, the purified product was formulated in 2.5 mL of saline solution containing 75 μL of ethanol. The specific activity ranged from 40 to 55 GBq/μmol at the end of synthesis with chemical purity based on UV absorption (254 nm) >95 % and the radiochemical purity was >99.5 % as determined by HPLC analysis.

Animals

Male Sprague–Dawley rats weighting 200–250 g (7–8 weeks old, n=3 for each set of *in vivo* experiments and n=4 for *in situ* experiments) were fasted for 24 h prior to the end of the experiment, and free access to water prior to the following experiments. All experimental protocols were approved by the Ethics Committee on Animal Care and Use of the center for molecular imaging science in RIKEN for PET study and by the Ethical Review Committee of Setsunan University for permeation study, and were performed in accordance with the Principles of Laboratory Animal Care (NIH publication No. 85–23, revised 1985).

Animal Study for PET Scan

The femoral vein of rats was cannulated with a polyethylene tube under anesthesia with a mixture of 1.5 % isoflurane before a day of the PET study. On the day of the experiment, rats were fixed with a retainer for small animals for imaging in an awake condition (Molecular Imaging Laboratory Inc., Osaka, Japan) for the following study. All PET scans were performed using microPET Focus 220 (Siemens, Knoxville, TN). Before emission scans, rats were placed in the center of the fields of views of microPET camera, and a transmission scan with rotating ^{68}Ge-^{68}Ga point source was performed for 25 min to reproduce the abdomen positioning and attenuation correction.

The concentration of radioactivity in [^{11}C]TEL solution for oral administration was set to 30–50 MBq/mL by adding appropriate volume of the saline (the concentration of [^{11}C]TEL was 0.25–0.50 μg/mL (0.49–0.99 μM)). At the start of the emission scan, [^{11}C]TEL solution was administered orally in doses of 70–100 MBq/kg. In addition, PET studies with [^{11}C]TEL in combination with non-radiolabeled telmisartan (0.5 and 10 mg/kg dose, completely dissolved into a solution with 1 v/v% of DMSO) were performed to investigate the changes in intestinal behavior as well as hepatobiliary transport when increasing the dose of non-radiolabeled telmisartan. PET data were taken in four parts as follows; scan #1) emission scan of abdominal region (0 to 30 min), scan #2) static scan of whole body (35 to 40 min), scan #3) emission scan of abdominal region (45 to 75 min) and scan #4) static scan of whole body (80 to 85 min). All emission scans were performed in 3D list mode. The data of first emission scan (scan #1) was sorted into a sinogram according to the following sequence: 20×15 s, 25×60 s. The data of second emission scan (scan #3) were sorted into sinograms for every 300 s. Whole-body scan with continuous bed motion (scan #2 and #4) was performed and the data were sorted into static sinograms. The blood was sampled via the cannulated femoral vain at 5, 10, 20, 30, 45, 60 and 90 min after administration. The volume of blood sampled at each time point was within 150 μL and the total blood volume sampled from one rat did not exceed 1.6 mL, about 10 % of total circulating blood volume.

Analysis of Luminal Contents After Oral Administration of Telmisartan

At 45 min after administration of [^{11}C]TEL with or without non-radiolabeled telmisartan, each rat was sacrificed and opened the abdominal cavity. Silicone tubes (i.d., 3 mm, o.d. 5 mm) were cannulated at both ends of duodenum and jejunum (5–10 cm from ligament of Treitz). Luminal solutions were collected by a slow infusion of appropriate volume of saline followed by air. Samples were deproteinized and supernatants were analyzed by HPLC-radiochromatography as shown in "Analysis of Radiolabeled Telmisartan and its Glucuronide."

Intestinal Absorption of Telmisartan in Rat

Intestinal absorption of telmisartan from rat intestine was evaluated by *in situ* closed loop method. Rats were

intraperitoneally anesthetized with pentobarbital. The abdominal cavity of rats was opened and an intestinal loop (length, 10 cm) was made at proximal jejunum by the cannulation with a silicone tube (i.d., 3 mm, o.d. 5 mm). Intestinal contents in the luminal side were removed by a slow infusion of appropriate volume of saline followed by air. The bile duct was also cannulated with a silicone tube (i.d., 0.8 mm, o.d. 1.2 mm). One mL of test solution, in which 0.1 mM (51.5 μg/mL) of telmisartan was prepared in saline with 1 v/v% of DMSO, was introduced into the intestinal loop and then both ends of the loop were closed. After predetermined time (5 or 10 min), the test solution in the loop was collected. The permeability of telmisartan was evaluated by the percentage of dose absorbed, by subtracting the remaining amount of the compound from the administered amount. The bile of rats treated with test solution for 10 min was collected from the cannulated tube for 20 min after test solution introduced into the loop.

In Vitro Membrane Transport Study

MDR1-MDCK II cells were cultured at 37 °C in a humidified air-5 % CO_2 atmosphere using MEMAM supplemented with 10 % FBS, 1 %L-glutamine, 1 % NEAA, and 0.5 % antibiotic-antimycotic mixture. Cells were routinely passaged by trypsin-EDTA when they became 90 % confluent. Cells were seeded on the cell culture inserts at a density of 2×10^5 cells/insert. Medium was replaced to fresh medium after 3 days. MDR1-MDCK II cell monolayers were ready for following transport studies 5 days after seeding.

MDR1-MDCK II cell monolayers were preincubated with transport medium (TM, Hanks' balanced salt solution with 25 mM HEPES, pH 7.4) for 20 min at 37 °C. After preincubation, transport studies were initiated by adding test solution of telmisartan to the donor side and TM with 1 v/v% DMSO to the receiver side. Drug transport study was performed at various concentrations of telmisartan from 1.0, 10 and 100 μg/mL (1.95, 19.5 and 195 μM) in TM with 1 v/v% DMSO and in apical-to-basal and basal-to-apical directions, and co-dosing of verapamil (0.1 mM), as a potent P-gp inhibitor, in the donor solution with test solution of telmisartan described above. Samples were taken from receiver solutions at an appropriate time point. All transport studies were performed under the no pH-gradient condition, pH 7.4 at apical and basal side, at 37 °C. The transepithelial electric resistance (TEER) of monolayers was monitored before and after the experiment, and there was no significant change in the TEER values during the experiment (data not shown).

Analytical Methods

Radioactivity in Blood Samples

The radioactivity in blood samples was counted by a gamma counter (1470 WIZARD® Automatic Gamma Counters, PerkinElmer, Waltham, MA). The radioactivity in each measured sample was corrected for the time decay from the point of [^{11}C]TEL administration.

Analysis of Radiolabeled Telmisartan and its Glucuronide

Luminal solutions (0.2 mL) from oral administration study with [^{11}C]TEL were mixed with acetonitrile (0.4 mL) and supernatants (0.5 mL) of each sample were taken. After removal of their solvent by evaporation, residues were dissolved in 0.2 mL of a mixture of 2 mM ammonium formate containing 0.1 v/v% formic acid (pH 3.0, solvent A) and acetonitrile (solvent B) (A/B=69/31, v/v). All treated samples were injected as 50–100 μL into the HPLC system. The reversed-phase HPLC system coupled with NaI (TI) positron detector (UG-SCA30, Universal Giken, Kanagawa, Japan) was conditioned using the mobile phases of initial composition (A/B=69/31, v/v). The column of 50×4.6(i.d.) mm filled with octadecylsilyl silica gel of 5 μm mean particle size (Waters Atlantis T3, Waters, MA) was used with a mobile phase consisting of solvent A and solvent B with gradient time period. The initial mobile phase was 69 % solvent A and 31 % solvent B pumped at a flow rate of 2.0 mL/min. Between 0.5 and 2.5 min, the percentage of solvent B was increased linearly to 80 %, where it was held for 1.5 min. At 4.0 min, the percentage of solvent B was decreased to 31 %. This condition was maintained until 6 min, at time when the next sample was injected into the HPLC system.

Analysis of Non-radiolabeled Telmisartan and its Glucuronide

Samples (0.1 mL) from *in situ* and *in vitro* experiments were mixed with acetonitrile (0.9 mL) and supernatants of each sample were analyzed according to the followings. Amounts of telmisartan and its glucuronide in the supernatant were determined by an UPLC system (ACQUITY® UPLC, Waters, MA) equipped with a tandem mass spectrometer (ACQUITY® TQD, Waters, MA). The reversed-phase Waters ACQUITY® UPLC BEH C18 analytical column of 50×2.1(i.d.) mm and 1.7 μm particle size (Waters, MA) was used with a mobile phase consisting of 0.1 v/v% formic acid in water (solvent A) and acetonitrile containing 0.1 v/v% formic acid (solvent B) with gradient time period. The initial mobile phase was 98 % solvent A and 2 % solvent B pumped at a flow rate of 0.3 mL/min. Between 0 and 1.0 min, the

percentage of solvent B increased linearly to 95 %, where it was held for 1.0 min. Between 2.01 and 2.5 min, the percentage of solvent B decreased linearly to 2 %. This condition was maintained until 3 min, at time when the next sample was injected into the UPLC system. All treated samples were injected as 5 μL into the UPLC system. Ionization conditions for analysis of telmisartan were as follows: electrospray ionization; positive mode; source temperature, 150 °C; desolvation temperature, 400 °C; cone voltage, 30 V; collision energy, 10 eV. Precursor and production ions (m/z) for detection of telmisartan with the retention time (RT) at 1.2 min were 515.62 and 193.14, respectively. The quantification of telmisartan-glucuronide was performed in the same procedure for telmisartan analysis (RT at 0.8 min), because telmisartan-glucuronide was dissociated into telmisartan and glucuronic acid by electrospray ionization. A standard curve was prepared for each compound and linearity ($r^2 > 0.999$) was observed at a concentration range of 0.02–100 ng/mL (0.04–195 nM).

Data Analysis

Image Analysis of Scan Data by microPET

All emission scan images were reconstructed with microPET manager (Siemens, Knoxville, TN). Image reconstruction was achieved by standard 2D filtered back projection (FBP) using Ramped filter 0.5 with cutoff at Nyquist frequency (0.5 cycle/pixel, defined as an upper frequency limit for the reconstruction filter in this study), or by maximum likelihood expectation maximization (MLEM). Compared with FBP, MLEM reconstructed images have been shown to result in improved spatial resolution and noise properties on small animal PET images, an advantage for image registration. Meanwhile FBP reconstructed images were used for quantification. Regions of interest (ROIs) were delineated in one slice for the stomach, the small intestine and the liver, and identified using PMOD 3.1 program (PMOD Technologies Inc., Zurich, Switzerland) according to previously described method (15,18). ROIs of each tissue in all slices were combined bilaterally and were changed to volumetric regions of interest (VOI). Defined VOIs of each tissue were applied to the FBP reconstructed images, and then the radioactivity in each tissue was calculated and was normalized to the administered dose (% of dose/tissue).

Assuming that gastric emptying follows the first-order rate kinetic, rate constants of gastric emptying was obtained by fitting the data of time-course of the radioactivity in the stomach to the first order kinetic model.

Intestinal Absorption of Telmisartan

The following equation was used to calculate the permeability (effective permeability coefficient; P_{eff}, cm/sec) to the intestinal membrane of rat proximal jejunum.

$$P_{eff} = \frac{k_a V}{2\pi RL}$$

where k_a is the absorption rate constant of the compound estimated from the percentage of dose absorbed during the defined period, assuming that the compound absorption follows the first-order rate kinetic. V is the volume of the solution introduced to the loop. L and R represent the length and the radius of the used the segment of intestinal loop, respectively, and thus the value of $2\pi RL$ corresponds to its surface area. As the radius of proximal jejunum, the value (0.18 cm) reported by Fagerholm *et al.* (19) was used.

In Vitro Membrane Permeability

The permeability (apparent permeability coefficient; P_{app}, cm/s) of telmisartan to MDR1-MDCK II cell monolayer under various conditions was calculated according to the following equation:

$$P_{app} = \frac{dQ}{dt} \times \frac{1}{A \times C_0}$$

where dQ/dt is the amount of drug transported within a given time period (μg/sec), A is the membrane surface area (0.9 cm^2), and C_0 (μg/mL) is the donor concentration at t=0. The permeability ratio was calculated using the following equation:

$$\text{Permeability ratio} = \frac{P_{app,\,BA}}{P_{app,\,AB}}$$

where $P_{app,\,AB}$ and $P_{app,\,BA}$ are the permeability of telmisartan in the absorptive (apical to basal) and secretive (basal and apical) direction, respectively.

Statistical Analysis

Data were presented as means with standard deviation (s.d.) for individual groups. Statistical significance was assessed with the unpaired Student's t-test and p values of 0.05 or less was considered significant.

RESULTS

In Vivo Oral Administration Study with PET

Whole-Body Distribution of Radioactivity

Maximum intensity projection (MIP) image of rat whole body on PET scan at 40 and 85 min after oral administration of [^{11}C]TEL at a tracer dose were shown in Fig. 2. As a reference, MIP images of [^{18}F]FDG at 85 min from our previous report (15) was attached together with the result of [^{11}C]TEL. Although the radioactivity after oral administration of [^{18}F]FDG distributed to the whole body, that of [^{11}C]TEL remained mostly in the gastrointestinal tract at both time points and was slightly detected in the liver. When [^{11}C]TEL with non-radiolabeled telmisartan was administered to rats, the radioactivity was also distributed into only abdominal region, irrespective of non-radiolabeled telmisartan dose (data not shown).

Dynamic MIP Images in the Abdominal Region After Oral Administration of [^{11}C]TEL on PET Study

Figure 3 shows the distribution of the radioactivity in the abdominal region of rat at 2, 5, 10, 20, 45 and 75 min after oral administration of [^{11}C]TEL with or without co-dosing of non-radiolabeled telmisartan. After [^{11}C]TEL was administered, the radioactivity was quickly excreted from the stomach to the small intestine, irrespective of the administered amount of non-radiolabeled telmisartan. After administration of tracer dose of [^{11}C]TEL, the radioactivity was retained mostly in the small intestine during PET scanning and was gradually accumulated into the liver. Co-administration of non-radiolabeled telmisartan decreased the radioactivity in the intestinal region, especially that in the proximal small intestine. This effect was dose-dependent and, with 10 mg/kg of non-radiolabeled telmisartan, the radioactivity in the proximal intestine disappeared quickly and high activity was detected in the liver at 20 min after administration.

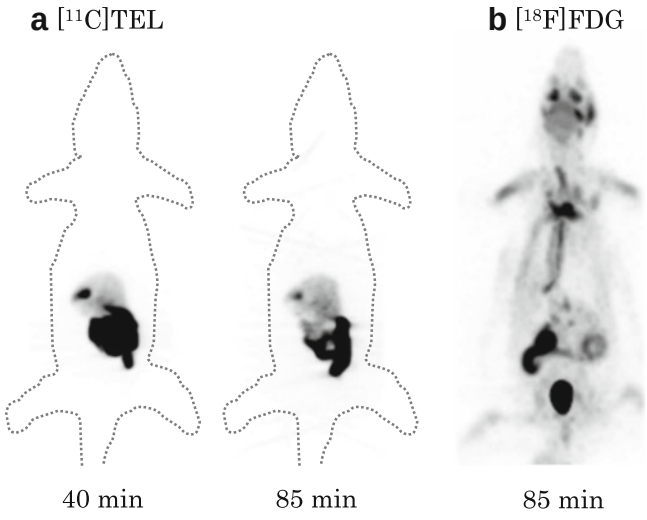

Fig. 2 PET images of whole body after oral administration of (**a**) [^{11}C]TEL and (**b**) [^{18}F]FDG. Coronal maximum intensity projecting PET images in the whole body were captured for (**a**) [^{11}C]TEL at 40 and 85 min and (**b**) [^{18}F]FDG at 85 min after administration taken from our previous report (15).

The time course of the fraction of radioactivity (% of dose) remained in the stomach and the small intestine after oral administration of [^{11}C]TEL was obtained from VOIs in each region and was shown in Fig. 4. The recovery of the total radioactivity in the stomach and small intestine immediately after the administration of [^{11}C]TEL was almost 80 % in all conditions. In the case of tracer dose of [^{11}C]TEL, most of the radioactivity in the stomach disappeared quickly after administration. Gastric emptying of the radioactivity delayed slightly with increasing the total dose of telmisartan. The rate constant of gastric emptying was calculated as 0.140 ± 0.042 min^{-1} for tracer dose, 0.118 ± 0.051 min^{-1} for 0.5 mg/kg dose, and 0.081 ± 0.027 min^{-1} for 10 mg/kg dose, although the difference was insignificant among three doses.

After administration of tracer dose or 0.5 mg/kg dose of telmisartan, the radioactivity in the small intestine sharply increased and reached a plateau level within 30 min (approximately 70 % of dose at tracer dose and 60 % at 0.5 mg/kg dose). When dose of co-administered telmisartan was increased to 10 mg/kg, increase in the intestinal radioactivity was slowed down and did not reach a plateau during the PET scanning. At the final time point of abdominal PET scanning (75 min), total radioactivity remained in the GI tract was about 70, 60, and 50 % of dose, respectively at tracer, 0.5 mg/kg and 10 mg/kg dose.

Analysis of the Radioactivity in the Liver

Figure 5 shows the time-course of the radioactivity in the liver. After oral administration of tracer dose of [^{11}C]TEL, the radioactivity gradually increased during first 30 min and reached only 0.7 % of dose. When [^{11}C]TEL was administered with 0.5 mg/kg of non-radiolabeled telmisartan, the radioactivity in the liver reached a peak (3 % of dose) within 10 min after administration. When the dose was increased to 10 mg/kg, the peak reached 17 % of dose at 20 min after administration. Pharmacokinetic parameters (C_{max}, T_{max}, AUC_{0-75}) for hepatic disposition of the radioactivity were calculated and summarized in Table I. Along with a increase in dose, C_{max} and AUC_{0-75} increased and T_{max} decreased. Compared to the tracer dose of [^{11}C]TEL, AUC_{0-75} with 0.5 mg/kg and 10 mg/kg of non-radiolabeled telmisartan became 10 and 50 times higher, respectively.

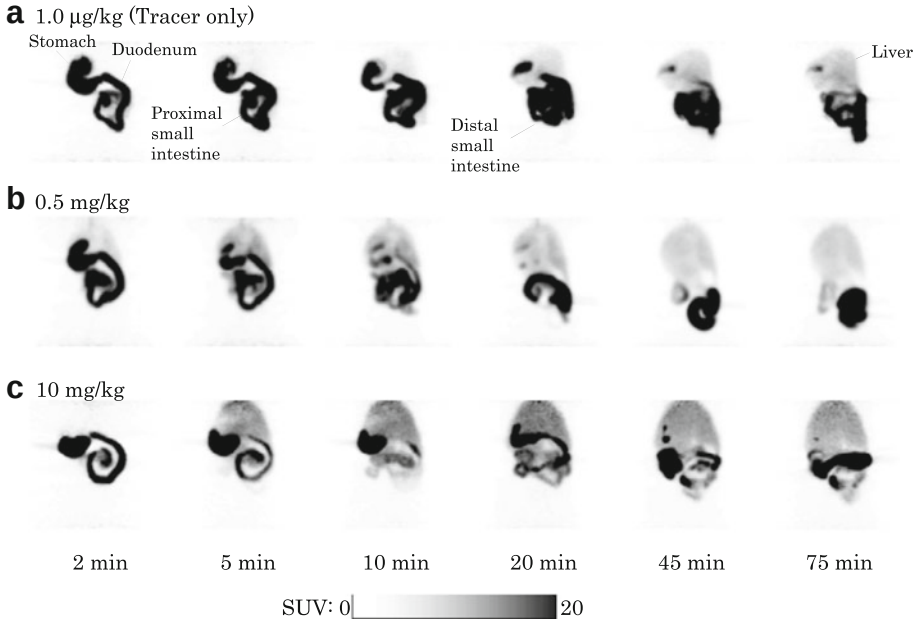

Fig. 3 Serial PET images of abdominal region acquired at each timepoint after oral administration of [^{11}C]TEL with or without non-radiolabeled telmisartan to rats. Coronal maximum intensity projecting PET images in the abdominal region were captured at 2, 5, 10, 20, 45 and 75 min following oral administration of [^{11}C]TEL (**a**) at tracer dose, (**b**) co-dosing with 0.5 mg/kg and (**c**) 10 mg/kg of non-radiolabeled telmisartan.

Analysis of the Radioactivity in the Blood Samples

Figure 6 shows the time-course of the radioactivity (% of dose/mL) in the whole blood after oral administration of [^{11}C]TEL with or without co-dosing of non-radiolabeled telmisartan. PK parameters were calculated from the time-course of the blood radioactivity and were summarized in Table II. After oral administration of [^{11}C]TEL, radioactivities in the whole blood reached to C_{max} within 20 min (T_{max}) in all dosage conditions. After administration with 0.5 and 10 mg/kg of non-radiolabeled telmisartan, systemic exposure of radioactivity (AUC_{0-90}) increased 4- and 10-folds compared to that at tracer dose, respectively.

Assessment of Radiometabolite Components in the Intestinal Luminal Contents

Figure 7 shows the radiochromatogram of intestinal luminal contents at 40 min after oral administration of [^{11}C]TEL with or without co-dosing of non-radiolabeled telmisartan. At tracer dose, half of the radioactivity was found to be derived from telmisartan and another half was from its O-acyl-glucuronide in both duodenum and jejunum (Fig. 7a). Increase in the dose of non-radiolabeled telmisartan caused the significant decrease in the fraction of telmisartan itself. At 10 mg/kg dose, most of luminal radioactivity was derived from O-acyl-glucuronide of telmisartan (Fig. 7b, c).

In Situ Intestinal Closed Loop Study

Intestinal absorption and metabolism of telmisartan were investigated by *in situ* closed loop method with proximal jejunum in rat. When 0.1 mM of telmisartan was applied into the intestinal loop as a solution, it was gradually absorbed and less than half of the applied amount remained in the intestine at 10 min. It suggests that the telmisartan has high absorbability from the intestine (Table III). Assuming that the absorption process of telmisartan follows the first-order rate kinetics, its permeability on the intestinal membrane was calculated to be $1.10 \pm 0.34 \times 10^{-4}$ cm/s. Amount of telmisartan-O-acyl-glucuronide, a major metabolite of telmisartan, in the luminal loop was also determined (Table III). At 10 min after administration, only 2 % of administered amount of telmisartan was detected as its glucuronide in the luminal solution.

During the loop experiment, bile juice was also collected to determine the amount of telmisartan and its glucuronide excreted into the bile (Table IV). Although the sum of excreted amount of telmisartan and its glucuronide showed large inter-individual deviations (3.78 to 13.03 nmol during 20 min), more than 90 % in the total excreted amount was found as telmisartan-O-acyl-glucuronide in all rats.

In Vitro Transcellular Transport Study with MDR1-MDCK II Cell Monolayers

The permeability of telmisartan across MDR1-MDCK II cell monolayer was determined in both absorptive (apical to basal) and secretive (basal to apical) directions. As shown in Fig. 8, the permeability in both directions was fluctuated by the initial donor concentration of telmisartan. The absorptive permeability gradually increased with increasing the donor concentration, whereas the secretive permeability dramatically decreased. The permeability ratio (secretive/absorptive permeability) at 1.0, 10 and 100 μg/mL (1.95, 19.5 and 195 μM) of telmisartan concentration was 13.6, 3.2 and 1.3, respectively.

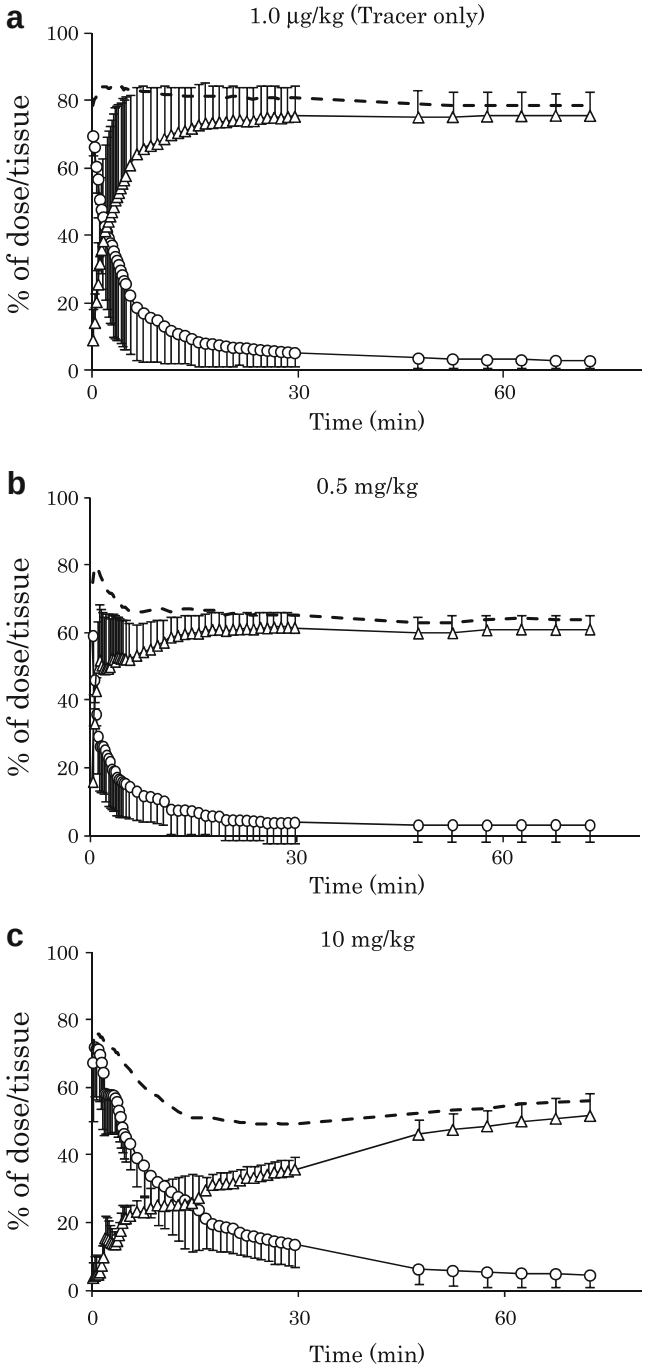

Fig. 4 Time-radioactivity curves in the stomach and the small intestine after oral administration of [^{11}C]TEL with or without non-radiolabeled telmisartan to rats. Symbols represent the percent of dose of the radioactivity in the stomach (○) and the small intestine (▵) after oral administration of [^{11}C]TEL (**a**) at tracer dose, (**b**) co-dosing with 0.5 mg/kg and (**c**) 10 mg/kg of non-radiolabeled telmisartan. Dotted lines represent the sum of radioactivities in the stomach and the small intestine. Data were expressed as % of the oral dose (% of dose/tissue). Each value represents the mean ± s.d. of three experiments.

Verapamil was used as a inhibitor of P-gp. When verapamil (100 μM) was added to the donor solution with telmisartan (1.0 μg/mL (1.95 μM)), absorptive permeability of

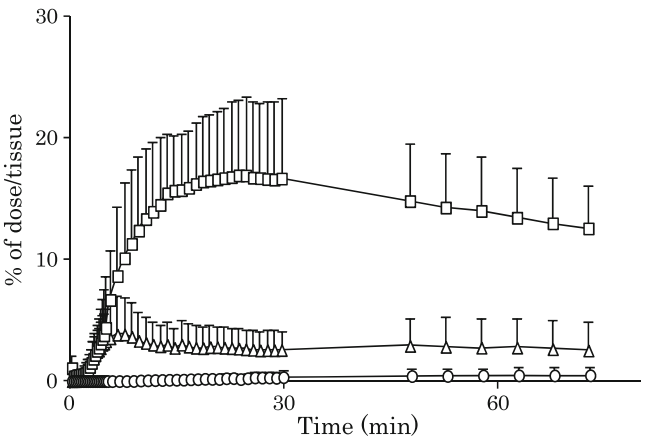

Fig. 5 Time-radioactivity curves in the liver after oral administration of [^{11}C]TEL with or without non-radiolabeled telmisartan to rats. Symbols represent the percent of dose of the radioactivity in the liver after oral administration of [^{11}C]TEL at tracer dose (○), co-dosing with 0.5 mg/kg (▵) and 10 mg/kg (□) of non-radiolabeled telmisartan. Data were expressed as % of the oral dose (% of dose/tissue). Each value represents the mean ± s.d. of three experiments.

telmisartan increased and secretive one decreased compared to those without verapamil. The permeability ratio was significantly decreased from 13.6 to 1.5 by the addition of verapamil to the donor solution.

DISCUSSION

In the clinical study, telmisartan was reported to show a non-linear pharmacokinetics after oral administration to humans (20). Both maximum concentration (C_{max}) and area under the concentration-time curve (AUC) of telmisartan in the plasma increase non-linearly with dose ranged from 20 to 120 mg, leading to a higher systemic exposure than that expected from the dose-proportional manner.

The systemic exposure of the radioactivity after oral administration of [^{11}C]TEL increased with increasing the dose of non-radiolabeled telmisartan, indicating the non-linear BA and/or PK of telmisartan in rats. In the clinical study, the T_{max} of telmisartan in human plasma was shortened when increasing the dose at around clinical dose (20–120 mg) (20). The T_{max} of the radioactivity was shortened at

Table I Pharmacokinetic Parameters of Hepatic Radioactivity after Oral Administration of Telmisartan to Rats

Dose (mg/kg)	T_{max} n.l. (min)	C_{max} n.l. (% of dose/tissue)	AUC_{0-75} (% of dose·min/tissue)
0.001	24.2 ± 2.5	0.48 ± 0.66	21.6 ± 31.2
0.5	40.2 ± 37.0	4.77 ± 2.87	195.6 ± 120.5
10	43.8 ± 33.8	17.06 ± 6.32	993.8 ± 349.9

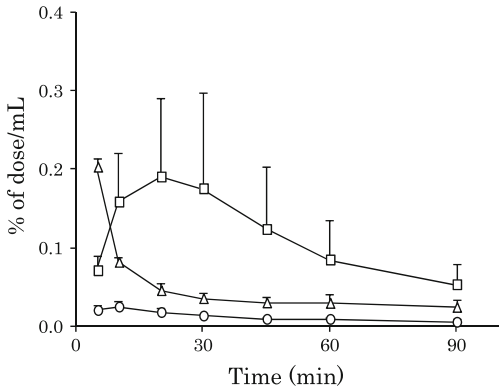

Fig. 6 Time-radioactivity curves of the whole blood after oral administration of [^{11}C]TEL with or without non-radiolabeled telmisartan to rats. Symbols represent the percent of dose of the radioactivity in the whole blood after oral administration of [^{11}C]TEL at tracer dose (○), co-dosing with 0.5 mg/kg (▵) and 10 mg/kg (□) of non-radiolabeled telmisartan. Data were expressed as % of the oral dose in whole blood (% of dose/mL). Each value represents the mean ± s.d. of three experiments.

0.5 mg/kg dose and was retarded at 10 mg/kg dose in the present study. The reason of this discrepancy at highest dose might be due to the decrease in the rate of intestinal absorption caused by the precipitation of telmisartan in the intestinal lumen. In our previous study, we have successfully demonstrated the high potency of PET imaging technology to visualize and kinetically analyze the process of oral drug absorption using [^{18}F]FDG as a model probe (15). Again in this study, PET imaging technology was utilized to elucidate the process of non-linear BA and/or PK of orally administered telmisartan.

After oral administration of [^{11}C]TEL at several dosing conditions, the radioactivity was rapidly discharged from the stomach to the small intestine. Gastric emptying rate of the radioactivity was not significantly affected by the co-administration of non-radiolabeled telmisartan. In contrast, PET scanning clearly demonstrated the effect of dose on the intestinal absorption of telmisartan and the subsequent distribution to the liver as follows:

1) when tracer amount of [^{11}C]TEL was administered, high level of radioactivity (approximately 80 % of dose) remained in the small intestine until the end of PET scan. The radioactivity component in the duodenum and the jejunum was derived almost equally from telmisartan and its O-acyl-glucuronide. Distribution of radioactivity to the liver was slow and was only less than 1 % of dose even at 60 min after administration.
2) when moderate dose (0.5 mg/kg) of non-radiolabeled telmisartan was co-administered with [^{11}C]TEL, the radioactivity in the intestine decreased to 70 % of dose and that in the liver increased to 4 % of dose at a peak. In the intestine, fraction of radioactivity derived from telmisartan decreased significantly.
3) when dose of non-radiolabeled telmisartan was increased to 10 mg/kg, intestinal radioactivity further decreased and that in the liver increased to 17 % of dose. In addition, the fraction of telmisartan in the intestine became very small and the most of radioactivity was derived from its O-acyl-glucuronide.

Table II Pharmacokinetic Parameters from Blood-Profile after Oral Administration of Telmisartan to Rats

Dose (mg/kg)	T_{max} n.l. (min)	C_{max} (% of dose/mL)	AUC_{0-90} (% of dose·min/mL)
0.001	10 ± 0[a]	0.024 ± 0.008	1.01 ± 0.09
0.5	5 ± 0[a]	0.202 ± 0.011	3.96 ± 0.73
10	20 ± 10	0.206 ± 0.107	10.15 ± 5.76

[a] No data variance

In order to understand the reason of the non-linearity in the intestinal absorption, hepatic accumulation, and systemic exposure of orally administered telmisartan, *in situ* and *in vitro* experiments with rat small intestine and cultured cell monolayers were conducted. In the intestinal absorption of telmisartan, following two processes are possible to be saturated when dose is increased, i.e. transporter mediated efflux and metabolism in enterocytes. As the metabolism process of telmisartan in rats, it is reported that telmisartan is readily glucuronidated in the liver and the intestine, however; it is not metabolized via Phase I reactions and is a subject to a considerable intestinal first-pass effect (21). Therefore, the cause of the changes in the radioactivity in the intestinal behavior and liver distribution may include the saturation of intestinal first pass effect when increasing telmisartan doses. Concerning the involvement of transporter mediated efflux process, telmisartan has been reported to inhibit P-gp-mediated efflux (22,23).

In the present study, *in vitro* results with MDR1-MDCK II cell monolayer that express human P-gp clearly indicated that telmisartan is also a good substrate of P-gp. In Fig. 8, 100 μg/mL concentration of telmisartan reduced the permeability ratio (basal to apical/apical to basal) to 1.3, showing the saturation of P-gp mediated efflux. In the PET study in rats, dose-concentration (dose/initial ingested water volume) of non-radiolabeled telmisartan was 0.25 and 5.0 mg/mL (0.49 and 9.7 mM) respectively for 0.5 mg/kg and 10 mg/kg dose. In addition, the IC_{50} value of telmisartan for inhibition of digoxin transport by P-gp across Caco-2 cell monolayer was reported to be 2.19 μM (22), which was significantly lower than that oral dose concentration at 0.5 and 10 mg/kg dose. Assuming that the affinity of telmisartan to P-gp on rat and human is similar, amount of non-radiolabeled telmisartan co-administered with [^{11}C]TEL is considered to be enough to saturate the P-gp mediated efflux in rat small intestine. Guo at al. and Miura *et al.* have

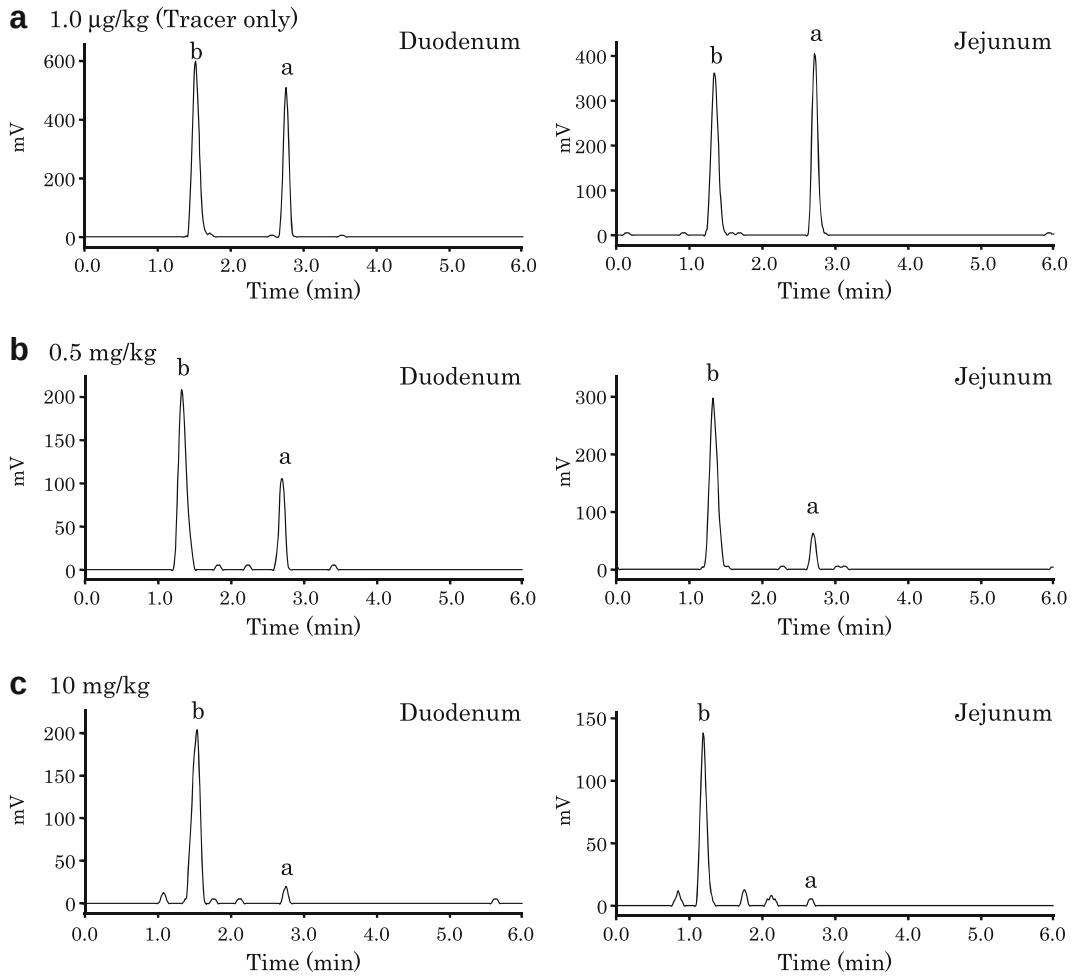

Fig. 7 Radiochromatograph of intestinal luminal contents after oral administration of [^{11}C]TEL with or without non-radiolabeled telmisartan to rats. Luminal contents in the duodenum and the jejunum after oral administration of [^{11}C]TEL (**a**) at tracer dose, (**b**) co-dosing with 0.5 mg/kg and (**c**) 10 mg/kg of non-radiolabeled telmisartan at 40 min were analyzed by radiochromatography. Peaks of (a) [^{11}C]telmisartan and (b) its glucuronide were identified using the retention time of each authentic standard sample.

revealed that MDR1 polymorphism does not affect pharmacokinetics of telmisartan at clinical dose (24,25), which could support our results.

In the *in situ* loop experiment, only a small amount of telmisartan-O-acyl-glucuronide was detected in the luminal solution (Table III), whereas glucuronide accounted for more than 90 % of excreted amount into the bile (Table IV). This result indicated that most of telmisartan-O-acyl-glucuronide detected in the intestinal lumen in the PET *in vivo* study was derived from the bile excretion.

Table III *In Situ* Evaluation of Intestinal Absorption and Metabolism of Telmisartan

Time (min)	Telmisartan n.l. (% of remaining[b])	Glucuronide[a] n.l. (% of appearance[c])
5	73.72 ± 9.60	1.17 ± 0.56
10	42.32 ± 5.87	2.07 ± 0.48

[a] Telmisartan-O-acyl-glucuronide

[b] Recovery of telmisartan in luminal solution

[c] % of glucuronide appearance on administered amount of telmisartan in luminal solution

It was suggested from both *in situ* and *in vitro* study that, when only a tracer dose of [^{11}C]TEL was administered, P-gp worked effectively as a barrier to prevent the absorption of telmisartan and the ratio of telmisartan in the total radioactivity in the luminal contents was kept relatively high. As the dose of telmisartan increased, the intestinal absorption of telmisartan increased due to the saturation of P-gp that resulted in the increase in the bile excretion of its glucuronide to the intestinal lumen. In the intestinal lumen, therefore, relative amount of telmisartan-O-acyl-glucuronide increased with dose.

In this case, it is also possible to consider that the increase in the uptake of telmisartan into enterocytes leads to the saturation of intestinal glucuronidation by UGTs, which may result in the higher exposure of telmisartan in the

Table IV Biliary Excretion of Telmisaltan and Its Glucuronide

Rat #	Telmisartan		Glucuronide[a]		Total[b]
	Excreted amount (nmol)	% of total excreted	Excreted amount (nmol)	% of total excreted	Excreted amount (nmol)
1	0.72	7.17	9.36	92.83	10.08
2	0.05	1.27	3.73	98.73	3.78
3	0.08	0.61	12.95	99.39	13.03
4	0.15	3.59	4.01	96.41	4.16
mean	0.25	3.16	7.51	96.84	7.76
s.d.	0.32	2.96	4.45	2.96	4.54

[a]Telmisartan-O-acyl-glucuronide

[b]Sum of excreted amounts of telmisartan and its glucuronide

portal vein and the systemic circulation. Since PET can detect only the sum of the radioactivity derived from the parent and its metabolites in the tissue, further studies should be performed for elucidating the effect of glucuronidation on the BA and/or PK of telmisartan directly in the present study where UGT-deficient animals such as gunn rat (UGT1 deficient rat) or UGT-specific inhibitors are utilized.

As shown in Fig. 5, time-profiles of the radioactivity in the liver were dose-dependent and, when the dose of co-dosed telmisartan was increased, the relative radioactivity (% of dose) in the liver dramatically increased. Dose-dependent increase in the radioactivity in the liver was more significant than that observed in the whole blood (compared by AUCs in Tables I and II). This result suggests the involvement of nonlinear mechanisms in the accumulation of radioactivity in the liver after oral administration of [^{11}C]TEL.

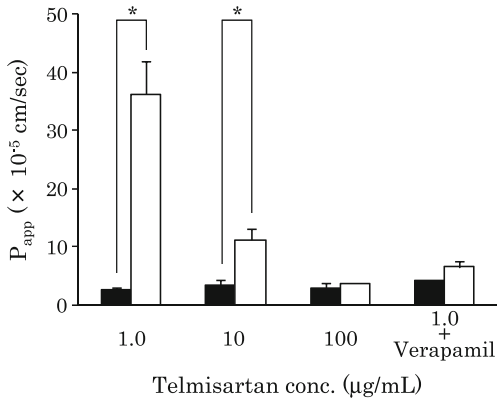

Fig. 8 Apparent permeability of telmisartan on transcellular transport study with MDR1-MDCK II cell monolayer. Apparent permeabilities of telmisartan on apical to basal (closed bars) and basal to apical (open bars) direction were measured at various donor concentrations (1.0, 10 and 100 μg/mL). In addition, 100 μM of verapamil was added into the donor solution at 1.0 μg/mL of telmisartan. Each value represents the mean ± s.d. of three experiments. Differences between apparent permeabilities on apical to basal and basal to apical directions at each conditions were statistically significant (*; $p < 0.05$).

The hepatobiliary transport of xenobiotics is coordinated by hepatic uptake and canalicular efflux processes. Various reports revealed that organic anion transporting peptides such as OATP1B1 and OATP1B3 are responsible for the hepatocellular uptake of organic anions. For the canalicular efflux of organic anions, ATP-binding cassette (ABC) transporters such as P-gp, canalicular multispecific organic anion transporter/multidrug resistance-associated protein 2 (cMOAT/MRP2) and breast cancer resistance protein (BCRP) play important roles. Telmisartan is a lipophilic compound with high log P value having both acidic and basic functional groups (10) and exists of anionic form in a solution at neutral pH (21). Ishiguro *et al.* have revealed that OATP1B3 was predominantly mediated the hepatocellular uptake of telmisartan *in vitro*. In addition, telmisartan was extensively glucuronidated in the liver and then its glucuronide was excreted into the bile by multispecific transporters including cMOAT/MRP2, P-gp and BCRP (10,11,26). In the previous report, Takashima *et al.* have reported that the *in vivo* hepatic uptake of telmisartan by OATP1B3 was saturated by increasing the dose administered intravenously, resulting the significant decrease in the systemic clearance by a PK analysis using PET technology (18).

Furthermore, they have calculated the ratio of parent/metabolite of telmisartan in the liver and the bile at a tracer and 10 mg/kg dose using a radiochromatography. In the liver, fraction of acyl-glucuronide was quite small (<9 % of total radioactivity) compared to telmisartan itself irrespective of the dose. This low fraction of acyl-glucuronide in the liver was kept constant during 40 min after IV injection of [^{11}C]TEL. In contrast, most of radioactivity in the bile was derived from the acyl-glucuronide (>89 % of total radioactivity) even at the higher dose. Assuming that the glucuronidation of TEL and the efflux of acyl-glucuronide into the bile occur sequentially in the liver, these results indicate that the process of glucuronidation rate-limits the biliary excretion of acyl-glucuronide of TEL.

Although the reasons of remarkable dose-dependency observed in the accumulation of radioactivity in the liver have not been fully clarified, together with the results in the

previous report, saturation of hepatic metabolism, acyl-glucuronidation, might be involved dominantly since this process rate limits the biliary excretion of the radioactivity. Consequently, at a high dose of telmisartan, higher systemic exposure than proportional increases in dose was achieved due to the saturation of P-gp mediated efflux in the intestine and OATP mediated uptake into the liver. At the same time, UGT mediated acyl-glucuronidation in the liver was saturated and higher accumulation of radioactivity was observed. In order to confirm these complicated processes of nonlinear PK of TEL, further studies such as an analysis of plasma and hepatic samples by fractionating radioactivity for metabolite (acyl-glucuronide) and unchanged drug at the end of *in vivo* PET study should be required and that will be reported as a next issue.

CONCLUSION

In this study, PET imaging analysis successfully demonstrated processes of intestinal absorption and hepatic distribution of telmisartan in rat. By combining with appropriate *in situ* and *in vitro* studies, saturable processes in the absorption/distribution of telmisartan were quantitatively analyzed and some factors causing its non-linear BA and PK were identified. Since PET imaging technology is non-invasive and applicable to human, this methodology is highly expected to be a potent tool for better understanding of GI absorption and subsequent tissue distribution of various drugs and drug candidates in the field of pharmaceutical research and drug development.

ACKNWLEDGMENTS AND DISCLOSURES

This study was done as a part of the Research Project for the "Establishment of Evolutional Drug Development with the Use of Microdose Clinical Trial" sponsored by the New Energy and Industrial Technology Development Organization (NEDO). We thank Mr. Masahiro Kurahashi of Sumitomo Heavy Industry Accelerator Service Ltd. for operation of the cyclotron and Ms. Emi Hayashinaka of the RIKEN Center for Molecular Imaging Science for the expert technical assistance. We also express our great appreciation to Boehringer Ingelheim Pharma KG for providing us *N*–desmethyl telmisartan (BIBT9584).

REFERENCES

1. Lipinski CA. Drug-like properties and the causes of poor solubility and poor permeability. J Pharmacol Toxicol Meth. 2000;44 (1):235–49.
2. Kola I, Landis J. Can the pharmaceutical industry reduce attrition rates? Nat Rev Drug Discov. 2004;3(8):711–5.
3. Ofer M, Wolffram S, Koggel A, Spahn-Langguth H, Langguth P. Modulation of drug transport by selected flavonoids: involvement of P-gp and OCT? Eur J Pharm Sci. 2005;25(2–3):263–71.
4. Kato Y, Miyazaki T, Kano T, Sugiura T, Kubo Y, Tsuji A. Involvement of influx and efflux transport systems in gastrointestinal absorption of celiprolol. J Pharm Sci. 2009;98(7):2529–39.
5. McClellan KJ, Markham A. Telmisartan. Drugs. 1998;56 (6):1039–44. discussion 1045–1046.
6. Stangier J, Su CA, Roth W. Pharmacokinetics of orally and intravenously administered telmisartan in healthy young and elderly volunteers and in hypertensive patients. J Int Med Res. 2000;28 (4):149–67.
7. Lo MW, Goldberg MR, McCrea JB, Lu H, Furtek CI, Bjornsson TD. Pharmacokinetics of losartan, an angiotensin II receptor antagonist, and its active metabolite EXP3174 in humans. Clin Pharmacol Ther. 1995;58(6):641–9.
8. Waldmeier F, Flesch G, Müller P, Winkler T, Kriemler HP, Bühlmayer P, De Gasparo M. Pharmacokinetics, disposition and biotransformation of [14C]-radiolabelled valsartan in healthy male volunteers after a single oral dose. Xenobiotica. 1997;27(1):59–71.
9. Stangier J, Schmid J, Türck D, Switek H, Verhagen A, Peeters PA, van Marle SP, Tamminga WJ, Sollie FA, Jonkman JH. Absorption, metabolism, and excretion of intravenously and orally administered [14C]telmisartan in healthy volunteers. J Clin Pharmacol. 2000;40 (12 Pt 1):1312–22.
10. Ishiguro N, Maeda K, Kishimoto W, Saito A, Harada A, Ebner T, Roth W, Igarashi T, Sugiyama Y. Predominant contribution of OATP1B3 to the hepatic uptake of telmisartan, an angiotensin II receptor antagonist, in humans. Drug Metabol Dispos. 2006;34 (7):1109–15.
11. Ishiguro N, Maeda K, Saito A, Kishimoto W, Matsushima S, Ebner T, Roth W, Igarashi T, Sugiyama Y. Establishment of a set of double transfectants coexpressing organic anion transporting polypeptide 1B3 and hepatic efflux transporters for the characterization of the hepatobiliary transport of telmisartan acylglucuronide. Drug Metab Dispos. 2008;36(4):796–805.
12. Nagata Y, Yamamoto K, Hiraoka M, Abe M, Takahashi M, Akuta K, Nishimura Y, Jo S, Masunaga S, Kubo S, *et al.* Monitoring liver tumor therapy with [^{18}F]FDG positron emission tomography. J Comput Assist Tomogr. 1990;14(3):370–4.
13. Bares R, Klever P, Hauptmann S, Hellwig D, Fass J, Cremerius U, Schumpelick V, Mittermayer C, Büll U. F-18 fluorodeoxyglucose PET *in vivo* evaluation of pancreatic glucose metabolism for detection of pancreatic cancer. Radiology. 1994;192(1):79–86.
14. Elsinga PH, Hendrikse NH, Bart J, Vaalburg W, van Waarde A. PET Studies on P-glycoprotein function in the blood–brain barrier: how it affects uptake and binding of drugs within the CNS. Curr Pharm Des. 2004;10(13):1493–503.
15. Yamashita S, Takashima T, Kataoka M, Oh H, Sakuma S, Takahashi M, Suzuki N, Hayashinaka E, Wada Y, Cui Y, Watanabe Y. Imaging of gastrointestinal absorption process of orally administered drugs using positron emission tomography. J Nucl Med. 2010;52(2):249–56.
16. Långström B, Antoni G, Gullberg P, Halldin C, Malmborg P, Någren K, Rimland A, Svärd H. Synthesis of L- and D-[methyl-^{11}C]methionine. J Nucl Med. 1987;28(6):1037–40.
17. Ferrieri RA, Garcia I, Fowler JS, Wolf AP. Investigations of acetonitrile solvent cluster formation in supercritical carbon dioxide, and its impact on microscale syntheses of carbon-11-labeled radiotracers for PET. Nucl Med Biol. 1999;26(4):443–54.
18. Takashima T, Hashizume Y, Katayama Y, Murai M, Wada Y, Maeda K, Sugiyama Y, Watanabe Y. The involvement of organic anion transporting polypeptide in the hepatic uptake of telmisartan in rats: PET studies with [(11)C]Telmisartan. Mol Pharm. 2011;8 (5):1789–98.

19. Fagerholm U, Lindahl A, Lennernäs H. Regional intestinal permeability in rats of compounds with different physicochemical properties and transport mechanisms. J Pharm Pharmacol. 1997;49(7):687–90.
20. Stangier J, Su CA, Schöndorfer G, Roth W. Pharmacokinetics and safety of intravenous and oral telmisartan 20 mg and 120 mg in subjects with hepatic impairment compared with healthy volunteers. J Clin Pharmacol. 2000;40(12 Pt 1):1355–64.
21. Wienen W, Entzeroth M, Van Meel JCA, Stangier J, Busch U, Ebner T, Schmid J, Lehmann H, Matzek K, Kempthorne-Rawson J, Gladigau V, Hauel NH. A review on telmisartan: a novel long-acting angiotensin II-receptor antagonist. Cardiovasc Drug Rev. 2000;18(2):127–56.
22. Kamiyama E, Nakai D, Mikkaichi T, Okudaira N, Okazaki O. Interaction of angiotensin II type 1 receptor blockers with P-gp substrates in Caco-2 cells and hMDR1-expressing membranes. Life Sci. 2010;86(1–2):52–8.
23. Weiss J, Sauer A, Divac N, Herzog M, Schwedhelm E, Böger RH, Haefeli WE, Benndorf RA. Interaction of angiotensin receptor type 1 blockers with ATP-binding cassette transporters. Biopharm Drug Dispos. 2010;31(2–3):150–61.
24. Guo X, Chen XP, Cheng ZN, Luo X, Guo R, Chen L, Chen J, Chen B, Peng J, Li YJ. No effect of MDR1 C3435T polymorphism on oral pharmacokinetics of telmisartan in 19 healthy Chinese male subjects. Clin Chem Lab Med. 2009;47(1):38–43.
25. Miura M, Satoh S, Inoue K, Saito M, Habuchi T, Suzuki T. Telmisartan pharmacokinetics in Japanese renal transplant recipients. Clin Chim Acta. 2009;399(1–2):83–7.
26. Nishino A, Kato Y, Igarashi T, Sugiyama Y. Both cMOAT/MRP2 and another unknown transporter(s) are responsible for the biliary excretion of glucuronide conjugate of the nonpeptide angiotensin II antagonist, telmisaltan. Drug Metab Dispos. 2000;28(10):1146–8.